Effect of CALIPSO cloud aerosol discrimination (CAD) confidence levels on observations of aerosol properties near clouds

Weidong Yang [1], Alexander Marshak [2], Tamás Várnai [3] and Zhaoyan Liu [4]

[1] Goddard Earth Science and Technology Center, University of Maryland at Baltimore County, Baltimore, MD 21228 USA.

Email: weidong.yang@nasa.gov

[2] NASA Goddard Space Flight Center, Greenbelt, MD 20771 USA.

Email: Alexander.marshak@nasa.gov

[3] Joint Center for Earth System Technology, University of Maryland Baltimore County, Baltimore, MD 21228 USA.

Email: tamas.varnai@nasa.gov

[4] National Institute of Aerospace, Hampton, Virginia, USA.

Email: zhaoyan.liu-1@nasa.gov

Abstract

CALIPSO aerosol backscatter enhancement in the transition zone between clouds and clear sky areas is revisited with particular attention to effects of data selection based on the confidence level of cloud-aerosol discrimination (CAD). The results show that backscatter behavior in the transition zone strongly depends on the CAD confidence level. Higher confidence level data has a flatter backscatter far away from clouds and a much sharper increase near clouds (within 4 km), thus a smaller transition zone. For high confidence level data it is shown that the overall backscatter enhancement is more pronounced for small clear-air segments and horizontally larger clouds. The results suggest that data selection based on CAD reduces the possible effects of cloud contamination when studying aerosol properties in the vicinity of clouds.

Keywords: backscatter enhancement, transition zone, twilight zone, CALIPSO, aerosol, remote sensing

1. Introduction

It is widely recognized that the characteristics of clear sky areas tend to change near clouds, creating transition zones between cloudy and clear areas. The transition zones are well known for their systematic enhancement of brightness or aerosols optical depth retrieved from satellites (Ignatov et al., 2005; Loeb and Manalo-Smith, 2005; Matheson et al., 2005; Zhang et al., 2005; Koren et al., 2007; Loeb and Schuster, 2008), airborne (Redemann et al., 2009; Su et al., 2008), or ground instruments (Koren et al., 2007). Such zones can extend from hundreds of meters up to tens of kilometers (Perry and Hobbs, 1996; Lu et al., 2003; Charlson et al., 2007; Koren et al., 2007).

Such systematic enhancements in the transition zones seem to imply changes of aerosol properties near clouds (Bar-Or et al., 2011, Koren et al., 2008a; Su et al., 2008; Clark et al., 2002; Hoppel et al., 1986). Examination of aerosol property variations in such zones would help improve our understanding of aerosol-cloud interactions and allow more accurate estimations of the direct and indirect effects of aerosols in radiative budgets and climate forcing (Koren et al., 2008b; Medeiros et al., 2008). However, artifacts inherent in satellite-based signal detection and processing can also contribute to the apparent enhancements. These artifacts include the blurring effects of imaging systems (Qiu et al., 2000), three-dimensional (3D) radiative effects (e.g., Wen et al., 2007; Marshak et al., 2008; Kassianov and Ovchinnikov, 2008) from adjacent clouds, and cloud contamination (Ignatov et al., 2005; Zhang et al., 2005). Clearly, eliminating or reducing the effects of these artifacts is needed for correct retrievals of near-cloud aerosol parameters.

The CALIOP (Cloud-Aerosol Lidar with Orthogonal Polarization) lidar onboard the

CALIPSO (The Cloud-Aerosol Lidar and Infrared Pathfinder Satellite Observation) satellite (Winker et al., 2007) is an active instrument and is impervious to the blurring effects and the 3D effects of adjacent clouds that influence passive remote sensing instruments. As a result, it is especially well-suited for studying aerosol-cloud interactions and aerosol properties in the transition zone. Using CALIPSO data, Tackett and Di Girolamo (2009) and Várnai and Marshak (2011a) have observed near-cloud backscatter enhancements in the transition zone free of the artifacts of passive instruments.

Yet, the acquired aerosol data can still be cloud contaminated even in the lidar data. This is because clouds normally have no clear boundaries. Large-eddy simulations (Charlson et al., 2007) have shown that activated droplets can inhabit in much larger areas than the areas normally called cloudy. As described in studies of large transition zones using AERONET and MODIS data (Koren et al., 2007) and studies of cloud fields (Charlson et al., 2007; Koren et al., 2009), undetected wispy clouds, together with hydrated aerosols, are major contributors to the enhancement phenomena. Like all other remote sensing instruments, the CALIOP's binary identification of cloudy and cloud-free pixels is based on thresholds that depend on instrument characteristics and algorithms. Naturally, this binary definition cannot fully represent the continuum from obviously cloudy to obviously clear areas. The attempt to unambiguously distinguish between clear and cloudy areas in remote sensing data therefore results in declaring some pixels clear even if they contain some clouds. Hence, cloud contamination is an unavoidable feature in any study of aerosol property variations using remotely sensed aerosol data near clouds.

To reduce the impact of cloud contamination, median values are used to characterize aerosol backscatter behaviors (Tackett and Di Girolamo, 2009; Várnai and Marshak, 2011a), because medians are less influenced than means by any extreme high backscatter values arising from cloud contamination. Still, the extent of undetected clouds affecting or masking features from "true" aerosols is unclear and should be a subject of further studies.

This paper examines CALIOP observations of near-cloud aerosol properties, especially in relationship to the CAD score in the aerosol layer product. As discussed in detail in Section 2, the CAD score provides a measure of the confidence for each identification made (Liu et al., 2009).

This paper also suggests that CAD can help reduce the possible impact of cloud contamination if only aerosol data with CAD values beyond a certain threshold is used. This threshold has to be carefully chosen based on the balance between the needs for capturing purely aerosol physics with less cloud contamination and for using all-encompassing aerosol datasets.

The paper is organized as follows: First, Section 2 discusses the physical meaning of CAD scores, then Section 3 describes the methodology used in this study. Next, Section 4 discusses CAD-dependent aerosol behaviors observed near clouds. Finally, Section 5 summarizes the results.

2. A brief overview of CAD scores

The operational CALIOP data processing algorithm determines the Cloud-Aerosol Discrimination (CAD) score using the equation

$$\mathrm{CAD}(X)=\frac{p_{\mathrm{cloud}}(X)-k\,p_{\mathrm{aerosol}}(X)}{p_{\mathrm{cloud}}(X)+k\,p_{\mathrm{aerosol}}(X)}\times 100\% \qquad (1)$$

where X is the array of input measurements (i.e., altitude, 532 nm lidar backscatter, and the ratio of backscatters at 1064 and 532 nm at 5 km horizontal resolution), p_{cloud} and p_{aerosol} are probability density functions (PDFs) for clouds and aerosol, respectively, and k is the ratio of occurrence frequencies of cloud and aerosol layers. Because CAD scores are positive when $p_{\mathrm{cloud}} > k\,p_{\mathrm{aerosol}}$ and negative when $p_{\mathrm{cloud}} < k\,p_{\mathrm{aerosol}}$, layers with a positive CAD score are classified as cloud, and layers with a negative CAD value are classified as aerosol. While the sign of CAD scores determines the type of a feature, the magnitude, which is essentially a probability difference, describes how much more likely the feature is to be of one type than of the other.

The probability-difference nature of CAD suggests us a view angle to look at the cloud contamination issues in the observations of transition zone using CALIOP lidar. For aerosols such as those in traditionally defined clear areas far away from the transition zone, their absolute CAD values are relatively large because of their distinct differences in their cloud/aerosol probabilities. For the undetected cloud fragments and large hydrated aerosols such as those in cloud-free areas of transition zones, their absolute CAD values should be relatively small because of the small difference in their cloud/aerosol probabilities. This tendency may be understood by considering a virtual

experiment of adding cloud droplets into an aerosol volume. The addition of cloud droplets into an aerosol volume would increase the weight of cloud property for that volume, causing p_{cloud} to increase in Eq. (1); aerosols contaminated by undetected clouds therefore tend to reduce probability difference or CAD value. This implies that using only aerosol data with high confidence values (large negative CAD scores) reduces cloud contamination by excluding some observations affected by cloud particles. From the other hand, using only high confidence data may exclude some large hydrated aerosol particles from the analyses.

3. Methodology

The main objective of this research is to improve our understanding of near-cloud aerosol behaviors by examining their dependence on associated CAD values. Specifically, the study examines the relationships between CAD scores and near-cloud aerosol parameters such as integrated attenuated total backscatter (γ'_{λ}) and integrated attenuated total color-ratio (χ'); in addition, it examines the way these relationships depend on the size of clear-air segments and the horizontal size of clouds.

The study has included the analysis of monthlong CALIOP Version 2 nighttime datasets from each of the four seasons. (The comparison between Versions 2 and 3 data is discussed in the Appendix). Due to the similarity of behaviors in all months, however, the paper only presents results for a single month ranging from March 9 to April 10, 2008. The study considers all data over oceans free of sea ice, but excludes data over land for simplicity in data interpretation and for some limited environmental similarity.

The methodology is similar to that of Várnai and Marshak (2011a). For this study, CALIOP Level 1 attenuated backscatter (γ'_{λ}) profiles are integrated from 90 m to 3 km above mean sea level at 333 m resolution, and values of integrated attenuated total color-ratio (χ') are computed as $\gamma'_{1064}/\gamma'_{532}$. We focus on low altitudes because low warm clouds have the strongest impact on aerosols though the results are close to those integrated to 15 km (Várnai and Marshak, 2011a). The analysis uses clear profiles that are identified as cloud free in both the 0.333 km and 1.0 km operational cloud layer products, and the CAD score reported in the 5 km aerosol layer product is used to sort data. A 333 m backscatter profile is selected and used if the following conditions are all met: (a) The height of nearest cloud top is below 3 km. (b) The height of the top aerosol layer in the profile is below 3 km. (c) The distance between the two neighboring cloud edges is greater than 5 km, except in Section 4.3.1 where the distance between two neighboring cloud is a variable.

Median values provide more accurate characterizations of data with large outliers and are used in the analysis of this paper. The uncertainties of median values are estimated using the bootstrapping algorithm (Efron and Gong, 1983).

4. Observations and results

To illustrate and understand the influence of CAD-based data selection, let us start by examining the correlations between CAD values and backscatter strengths for two distance ranges from cloud edges, 0.33-7.0 km and 7.0-20 km (Figure 1). The results

show three notable tendencies. First, backscatter is higher closer to clouds. Earlier studies (e.g., Tackett and Di Girolamo 2009; Koren et al. 2007) attributed such higher backscatter values near clouds to processes such as aerosols swelling in the humid air around clouds, and to the increased presence of undetected cloud particles near clouds. Second, the attenuated backscatter γ'_{532} decreases with increasing confidence levels, especially for CAD scores beyond -60. The decrease can be explained by the fact that aerosol layers are identified with a higher confidence if backscatter is low, because clouds tend to be optically thicker than aerosols. Third, the backscatter enhancement near clouds decreases for increasing confidence levels (Figure 1b). This occurs because much of the enhancement comes from swollen aerosols and undetected cloud drops, and neither of these is too frequent in high-confidence aerosol data, given that large particle size of swollen aerosols and cloud drops reduces aerosol detection confidence.

4.1. Number of lidar profiles with high confidence aerosol detection

Figure 2 examines the number of cloud-free 333 m-resolution lidar profiles that contain aerosol layer(s) detected in six CAD ranges. The six CAD ranges are selected arbitrarily, to characterize γ'_{532} behaviors that change with CAD for CAD values beyond -60 (Figure 1a.). Figure 2a reveals that profile numbers increase near clouds for all six CAD ranges. This occurs because both short and long cloud-free segments yield profiles that are close to clouds, but only the (fewer) long cloud-free segments can yield profiles that are far away from clouds.

In contrast, Figure 2b shows that the fraction of profiles with high confidence aerosol

detections decreases near clouds dramatically. For example, aerosol detection confidence reaches the highest maximum level (-99, -100) for 50% of clear profiles far away from clouds, but only for 30% close to clouds. Naturally, this implies that relatively more low confidence aerosols are detected near clouds than far away from clouds. The decreasing ratio of high confidence data near clouds indicates that the properties of aerosols become more similar to those of clouds when cloud edges are approached. This can be explained by the swelling of hydrated aerosols and/or cloud-contamination near clouds, and can provide a different perspective for understanding the characteristics of the transition zone.

4.2. CAD dependent backscatter and color ratio enhancements near clouds

In this section we further examine the dependence of integrated attenuated backscatter γ'_{532} and color ratio χ' on CAD score.

Figure 3a shows γ'_{532} as a function of distance to clouds for six CAD ranges. In agreement with Figure 1 and with previous studies (Tackett and Di Girolamo, 2009; Várnai and Marshak, 2011a), the figure shows that integrated attenuated backscatter is enhanced near clouds. The results also agree with Figure 1 in that higher confidence data tends to have lower backscatter values. In addition, the figure indicates that in comparison to all aerosol data, high confidence data are flatter far away from clouds and have larger enhancements close to clouds. For example, between 5 km and 20 km the enhancement for the highest confidence data ($-100 < CAD < -99$) is only about 1/3 of the enhancement for all data ($-100 < CAD < 0$), whereas between 333 m and 5 km it is 1.7 times the value for all data.

Similar features also appear for attenuated total color ratios (Figure 3b). As seen in Figure 3b, χ' values for all CAD ranges increase as the distance to cloud decreases, indicating that aerosol size and/or concentration generally increase near clouds. High confidence level data (with large values of |CAD|) tends to have lower color ratios, because of the exclusion of highly humidified aerosols and cloud droplets that are large in size and result in low |CAD| scores. Moreover, the rate of color ratio increase far away from clouds (x > 5 km) is only about half as big for high confidence data as that for all data without CAD selection, whereas near clouds (x < 5 km) this rate is about twice as big for high confidence data as that for all data without CAD selection.

Such new features regarding CAD-dependent variations in backscatter γ'_{532} and attenuated color-ratio χ' are especially important because they may lead to different interpretations of the observed aerosol data and to different retrieved aerosol parameters. We note that, on one hand, excluding low-confidence aerosol data makes a dataset less comprehensive as some data from cloud-like larger aerosol particles may also be excluded; on the other hand, results derived from the high-confidence data are more clearly representative of only aerosols, without significant interference from undetected cloud particles.

A remarkable new finding seen in Figure 3a is the sharp increase in the near-cloud enhancement in γ'_{532} and χ' for the highest confidence level aerosol data. Considering that aerosol physical/optical properties are the most distinct from those of clouds for the highest confidence level aerosol data (CAD scores between -99 and -100), the sharp

enhancement observed for the highest confidence data is likely the most representative of aerosol property variations, with the least effect from undetected cloud fragments. This would also imply that particle size and/or concentration increase near detected clouds more gradually for undetected cloud particles than for aerosol particles.

4.3 Effects of cloud separation distance and cloud size

4.3.1 Effects of distance between clouds

Let us examine the dependence of aerosol properties near clouds on the distance between neighboring clouds (i.e., the lengths of clear-air segments). Figure 4 shows the relative enhancement of attenuated backscatter γ'_{532} as a function of distance to clouds for minimum cloud separation distances of 3 km, 11 km, and 35 km for all aerosol data (Figure 4a) and for the highest confidence data (Figure 4b). For the sake of convenience, our comparisons use a normalized backscatter, $R_t(x) = \gamma'_{532}(x)/\gamma'_{532}(20\text{ km})$, instead of $\gamma'_{532}(x)$. This comparison assumes that aerosols more than 20 km away from clouds are less affected by clouds (e.g., Twohy et. al., 2009).

There are some remarkable features in Figure 4. First of all, backscatter enhancements are more pronounced in cloud fields with smaller distances between neighboring clouds. This behavior is likely the result of correlations between relative humidity and the size of clear-air segments. Large areas of clear sky are usually associated with local high atmospheric pressure and relatively dry air in which aerosols have less chance to become highly humidified.

For further examination, we define the size of a transition zone as the distance to cloud x where $R_t(x)$=1.05. The size of transition zones for the all data cases (Figure 4a) are 1.0 km, 5.0 km and 7.0 km for the red, blue and black curves, respectively. These are much larger than their high confidence data counterparts: 0.6 km, 2.0 km and 3.0 km (Figure 4b). In addition, the most pronounced backscatter enhancements occur within 4 km from clouds for the high confidence data case whereas for the 'all aerosol' case, noticeable enhancements start farther.

The reduction of the size of transition zones between cloudy and cloud-free areas is a direct result of using only highest confidence aerosol data. In fact, the spatial extent of the transition zone is determined physically by the characteristics of clouds and their environment (Koren et al., 2007). Cumulus clouds, for example, may produce very different transition zones during different stages of their lifetime. During cloud formation, transition zones are usually smaller, because of the drying air produced by the downdraft just outside cloud boundaries. After clouds are fully developed, they start dissipating and produce a greatly extended transition zone that contains a mix of highly humidified aerosols and evaporating cloud droplets. Our CALIOP aerosol data includes samples from all cloud forming and dissipating stages and therefore should have a fairly large transition zone, as shown in Figure 4a. In contrast, the high confidence level cases with smaller transition zones in Figure 4b are likely associated with clouds in the forming stages, where the environment is relatively dry (Koren et al., 2007).

The most pronounced backscatter enhancements observed within 5 km to clouds for the highest confidence data (Figure 4b) mostly reflect the aerosol swelling effects in high relative humidity (RH) near clouds, with the least cloud contamination effect. In study of the effect of RH changes on the aerosol scattering near cloud, Twohy et al. (2009) found a 35% – 65% scattering enhancement between 20 km and cloud edge, with more than 2/3 of the increase occurring within 4 km to clouds. In addition, 26% - 30% of backscatter enhancement was observed within 5 km to clouds in the study of aerosol-cloud interactions using the High-Spectral-Resolution Lidar (HSRL) data over US east coast areas (Su et al., 2008). In contrast, backscatter enhancements in Figure 4b are about 6%, 12.5% and 24% for different distances between clouds. The discrepancies with aircraft measurements are partly due to the different time and locations of measurements, as well as atmospheric attenuations and molecular scattering being included in Figure 4. (Note that the information about distance between clouds in aircraft measurements was not available).

4.3.2 Effects of cloud horizontal size

This subsection examines the relationship between near-cloud backscatter behavior and cloud horizontal size. It compares near-cloud properties for three cloud size ranges: 1-2 km, 2-15 km, and greater than 15 km. Because high confidence aerosol data is less affected by cloud contamination and is more representative of aerosol particles, only highest confidence data with CAD=(-99, -100) is analyzed. Figure 5 presents γ'_{532} vs. distance to cloud relations for the three ranges of cloud horizontal size. The figure shows that the attenuated backscatter γ'_{532} behaves similarly for all three cloud-size ranges, with

slight differences near clouds. Noticeable differences in γ'_{532} occur mostly within 1-2 km from cloud edges, with γ'_{532} being slightly (~6%) smaller near small clouds. This result shows that horizontally larger clouds tend to have slightly stronger influences on aerosols in the surrounding air (perhaps because large convective clouds often have a greater vertical extent and can impact a thicker atmospheric layer than small convective clouds), but the large-scale meteorological conditions supporting large or small clouds do not strongly affect much on the aerosol behaviors near clouds.

Finally, we note that clouds outside the lidar track can also influence the observed areas, and their influence can be mistakenly accounted for the contributions from clouds on the track. The errors caused by this flaw have been analyzed by a simple random cloud field simulation (Tackett and Girolamo, 2009) and estimated by collocated CALIOP and MODIS observations (Várnai and Marshak, 2011b). Both results show that including the off-track clouds does not affect the general near-cloud trend while only correct the specific values.

5. Summary

This paper examines near-cloud behaviors of lidar backscatters using CALIOP data of various confidence levels defined by Cloud-Aerosol Discrimination (CAD) scores. The results show that, in consistence with previous studies, lidar backscatter is enhanced near clouds. At the same time, the fraction of high confidence aerosol detections decreases near cloud edges. The results also indicate that parts of the backscatter enhancements come from lower confidence level data that may be cloud contaminated to some extent.

The results also imply that using only high confidence level data reduces the impact of cloud contamination.

In particular, farther away from clouds enhancement rates (gradients of attenuated backscatter with respect to horizontal distance) are smaller for high confidence level data than for all data, whereas closer to clouds enhancement rates tend to be much greater for high confidence level data than for all data. As a result, highest confidence level aerosol data yields a much narrower and sharper transition zone near clouds than the full dataset does. This difference between the behaviors of all data and high confidence level data can lead to significant differences in the interpretation of backscatter data and in retrieved aerosol parameters.

The results for the highest confidence level data also show that near-cloud backscatter enhancements depend on the size of clear-air segments between neighboring clouds. It was found that the backscatter enhancement is lower for larger clear-air segments, which may reflect the fact that the air tends to be dryer in larger clear sky patches. In addition, while the near-cloud enhancements generally do not depend on cloud size, enhancements within 1-2 km of cloud edges are slightly stronger near larger clouds.

Acknowledgements

We gratefully acknowledge support for this research by the NASA Radiation Sciences Program and the CALIPSO/CLOUDSAT science team.

Appendix

A comparison of near-cloud behaviors based on CAD Versions 2 and 3

The CALIPSO cloud and aerosol discrimination (CAD) algorithm is probability based. A classification decision is made depending on what event (cloud or aerosol) is more likely to occur for a given set of measured parameters. Specifically, Eq. (1) is used for classification decisions. The PDFs in Eq. (1) are developed based on expert evaluations of lidar measurements for a global dataset (Liu et al., 2009). There is an overlap in the cloud and aerosol PDFs in parameter space where both aerosol and cloud can be possibly present. Outside the PDF overlap region where only cloud or aerosol can be present, a correct classification can be accurately made. Within the overlap region, a classification can still be made, but misclassifications will occur.

Version 2 (V2) of the operational CALIOP data processing algorithm uses three-dimensional (3D) PDFs (as functions of backscatter, color ratio, and altitude) (Liu et al., 2009) while Version 3 (V3) uses five-dimensional (5D) PDFs (also considering two additional parameters, depolarization and latitude) (Liu et al., 2010). In this 5D space, clouds and aerosols separate better and the PDF overlap region becomes smaller than in the 3D space. Therefore, the classification of clouds and aerosols has been improved, especially for dense dust layers that can be misclassified as cloud over/near the source regions in the Version 2 release (Liu et al., 2010).

However, the V3 CAD does not behave as expected near clouds. As shown in Figure A1, the fraction of high confidence samples of V3 cloud-free profiles generally increases approaching cloud whereas the same fraction in V2 decreases remarkably as seen in

Figure 2b. We do not understand this V3 CAD behavior yet. We note, however, that in the 5D space, the overlap region between clouds and aerosols is greatly reduced. The developed 5D PDFs used to calculate the CAD score may not be accurate enough to represent well the reduced overlap region. That is, although a better classification has been achieved by using 5D algorithm in the V3 release, the CAD score values near clouds may not be accurate enough due to attenuation by overlying layers or an inadequate correction for the overlying layers (Liu et al., 2010).

References

Bar-Or, R. Z., Altaratz, O., Koren, I., 2011. Global analysis of cloud field coverage and radiative properties, using morphological methods and MODIS observations. Atmos. Chem. Phys., 11, 191-200.

Clarke, A. D., Howell, S., Quinn, P. K., Bates, T. S., Ogren, J. A., Andrews, E., Jefferson, A., Massling, A., 2002. INDOEX aerosol: A comparison and summary of chemical, microphysical, and optical properties observed from land, ship, and aircraft. J. Geophys. Res. 107(D19), 8033.

Efron, B., Gong, G., 1983. A leisurely look at the bootstrap, the jackknife, and cross-validation. The American Statistician 37, 36-48.

Holben, B. N., Eck, T. F., Slutsker, I., Tanré, D., Buis, J. P., Setzer, A., Vermote, E., Eeagan, J. A., Kaufman, Y. J., Nakajima, T., Lavenu, F., Jankowiak, I., Smirnov, A., 1998. AERONET—A federated instrument network and data archive for aerosol characterization. Remote Sens. Environ. 66, 1–16.

Hoppel, W. A., Frick, G. M., Larson, R. E., 1986. Effect of nonprecipitating clouds on the aerosol size distribution in the marine boundary layer. Geophys. Res. Lett. 13, 125–128.

Ignatov, A., Minnis, P., Loeb, N., Wielicki, B., Miller, W., Sun-Mack, S., Tanre, D., Remer, L., Laslo, I., Geier, E., 2005. Two MODIS aerosol products over ocean on the Terra and Aqua CERES SSF. J. Atmos. Sci. 62, 1008–1031.

Kassianov, E.I., Ovtchinnikov, M., 2008. On reflectance ratios and aerosol optical depth retrieval in the presence of cumulus clouds. Geophy. Res. Lett. 35, L06311.

Koren, I., Remer, L. A., Kaufman, Y. J., Rudich, Y., Martins, J. V., 2007. On the twilight zone between clouds and aerosols. Geophys. Res. Lett. 34, L08805.

Koren, I., Martins, J. V., Remer, L. A., Afargan, H., 2008a. Smoke invigoration versus inhibition of clouds over the Amazon. Science 321, 946–949.

Koren, I., Oreopoulos, L., Feingold, G., Remer, L. A., Altaratz, O., 2008b. How small is a small cloud?. Atmos. Chem. Phys. 8, 3855–3864.

Koren, I., Feingold, G., Jiang, H., Altaratz, O., 2009. Aerosol effects on the inter-cloud region of a small cumulus cloud field, *Geophys. Res. Lett.*, *36*, L14805.

Liu, Z., Vaughan, M., Winker, D., Kittaka, C., Getzweich, B., Kuehn, R., Omar, A., Powell, K., Trepte, C., Hostetler, C., 2009. The CALIPSO lidar cloud and aerosol discrimination: Version 2 algorithm and initial assessment of performance. J. Atmos. Oceanic Technol. 26, 1198–1213.

Liu, Z., Kuehn, R., Vaughan, M., Winker, D., Omar, A., Powell, K. , Trepte, , Hu, Y., Hostetler, C., 2010. The CALIPSO cloud and aerosol discrimination: Version 3 algorithm and test results. http://www.calipso.larc.nasa.gov/resources/pdfs/ILRC_LaRC_2010/Liu_ILRC25_2010.pdf

Loeb, N. G., Manalo-Smith, N., 2005. Top-of-atmosphere direct radiative effect of aerosols over global oceans from merged CERES and MODIS observations. J. Climate 18, 3506–3526.

Loeb, N. G., Schuster, G. L., 2008. An observational study of the relationship between cloud, aerosol and meteorology in broken low-level cloud conditions. J. Geophys. Res. 113, D14214.

Lu, M. L., Wang, J., Freedman, A., Jonsson, H. H., Flagan, R. C., McClatchey, R. A., Seinfeld, J. H., 2003. Analysis of humidity halos around trade wind cumulus

clouds. J. Atmos. Sci. 60, 1041–1059.

Marshak, A., Wen, G., Coakley Jr., J. A., Remer, L. A., Loeb, N. G., Cahalan, R. F., 2008. A simple model for the cloud adjacency effect and the apparent bluing of aerosols near clouds. J. Geophys. Res. 113, D14S17.

Matheson, M. A., Coakley Jr., J. A., Tahnk, W. R., 2005. Aerosol and cloud property relationships for summertime stratiform clouds in the northeastern Atlantic from AVHRR observations. J. Geophys. Res. 110, D24204.

Medeiros, B., Stevens, B., Held, I. M., Zhao, M., Williamson, D. L., Olson, J. G., Bretherton, C. S., 2008. Aquaplanets, climate sensitivity, and low clouds. J. Clim. 21, 4974–4991.

Perry, K. D., Hobbs, P. V., 1996. Influences of isolated cumulus clouds on the humidity of their surroundings. J. Atmos. Sci. 53, 159–174.

Qiu, S., Godden, G., Wang, X., Guenther, B., 2000. Satellite-Earth remote sensor scatter effects on Earth scene radiometric accuracy. Metrologia 37, 411-414.

Redemann, J., Zhang, Q., Russell, P. B., Livingston, J. M., Remer, L. A., 2009. Case Studies of Aerosol Remote Sensing in the Vicinity of Clouds. J. Geophys. Res. 114, D6.

Smirnov, A., Holben, B. N., Kaufman, Y. J., Dubovik, O., Eck, T. F., Slutsker, I., Pietras, C., Halthore, R., 2002. Optical Properties of Atmospheric Aerosol in Maritime Environments. J. Atm. Sci. 59, 501-523.

Su, W., Schuster, G. L., Loeb, N. G., Rogers, R. R., Ferrare, R. A., Hostetler, C. A., Hair, J. W., Obland, M. D., 2008. Aerosol and cloud interaction observed from high spectral resolution lidar data. J. Geophys. Res. 113, D24202.

Tackett, J. L., Girolamo, L. D., 2009. Enhanced aerosol backscatter adjacent to tropical trade wind clouds revealed by satellite-based lidar. Geophys. Res. Lett. 36, L14804.

Twohy, C. H., Clement, C. F., Gandrud, B. W., Weinheimer, A. J., Campos, T. L., Baumgardner, D., Brune, W. H., Faloona, I., Sachse, G. W., Vay, S. A., Tan, D., 2002. Deep convection as a source of new particles in the midlatitude upper troposphere. J. Geophys. Res. 107(D21), 4560.

Twohy, C. H., Coakley Jr., J. A., Tahnk, W. R., 2009. Effect of changes in relative humidity on aerosol scattering near clouds. J. Geophys. Res. 114, D05205.

Várnai, T., Marshak, A., 2011a. Global CALIPSO observations of aerosol changes near clouds. IEEE Rem. Sens. Lett. 8, 19-23.

Várnai, T., and Marshak, A., 2011b. Analysis of co-located MODIS and CALIPSO observations near clouds. Atmos. Meas. Tech., in review

Vaughan, M. A., Winker, D. M., Powell, K. A., 2005. CALIOP Algorithm Theoretical Basis Document Part 2: Feature Detection and Layer Properties Algorithms,(ATBD), p20, Rel. 1.01. Sept. 27, 2005, http://www-calipso.larc.nasa.gov/resources/pdfs/PC-SCI-202_Part2_rev1x01.pdf

Wen, G., Marshak, A. Cahalan, R. F., Remer, L. A., Kleidman, R. G., 2007. 3-D aerosol-cloud radiative interaction observed in collocated MODIS and ASTER images of cumulus cloud fields. J. Geophys. Res. 112, D13204.

Winker, D. M., Hunt, W., McGill, M., 2007. Initial performance assessment of CALIOP. Geophys. Res. Lett. 34, L19803.

Zhang, J., Reid, J. S., Holben, B. N., 2005. An analysis of potential cloud artifacts in MODIS over ocean aerosol optical thickness product. Geophys. Res. Lett. 32, L15803.

Figures

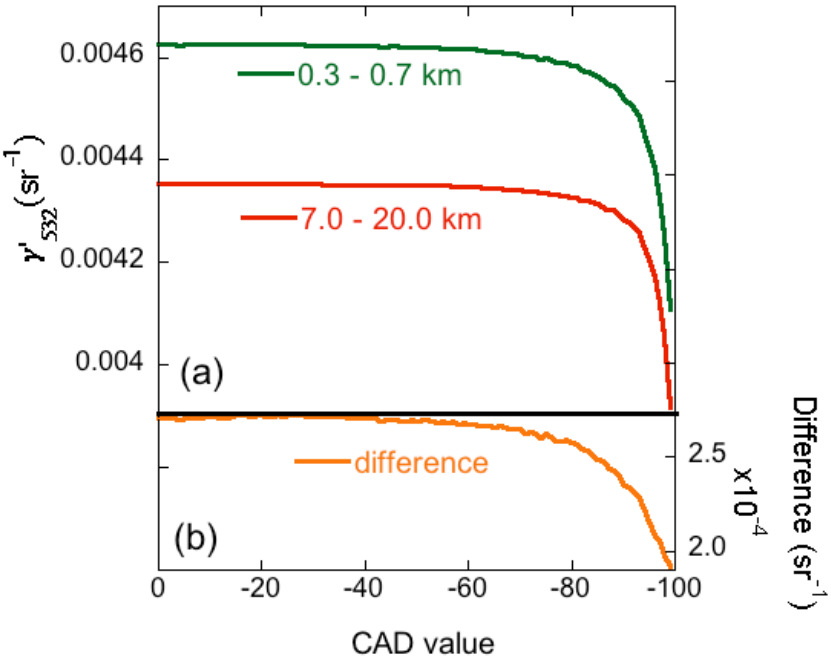

Figure 1. Effects of CAD-based data selection on the median attenuated total 532 nm backscatter, γ'_{532}, integrated up to 3 km altitude for two ranges of distance to nearest cloud: from 0.3 km to 7.0 km and from 7.0 km to 20.0 km (a) and their difference (b).

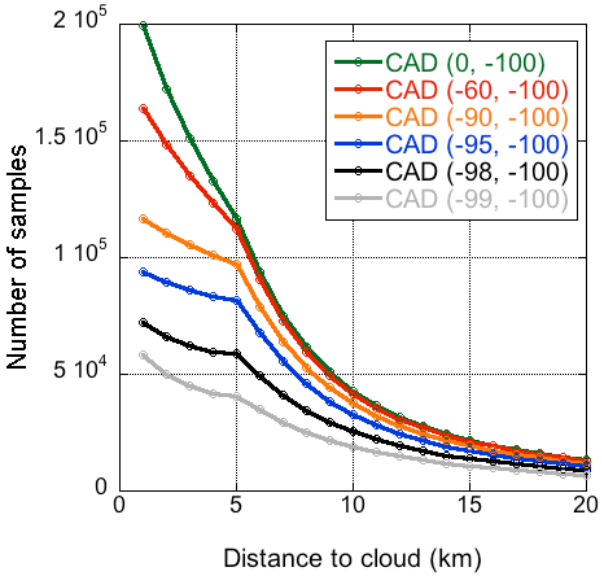

(a)

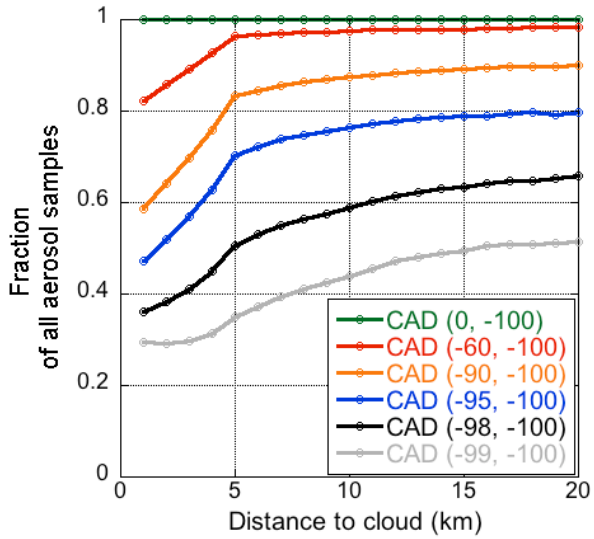

(b)

Figure 2. Effects of CAD on the number of aerosol samples. (a) Number of samples under different CAD score criteria and (b) their corresponding fractions over the total number of aerosol samples. The break near 5 km is due to the exclusion of data from clear-sky segments shorter than 5 km.

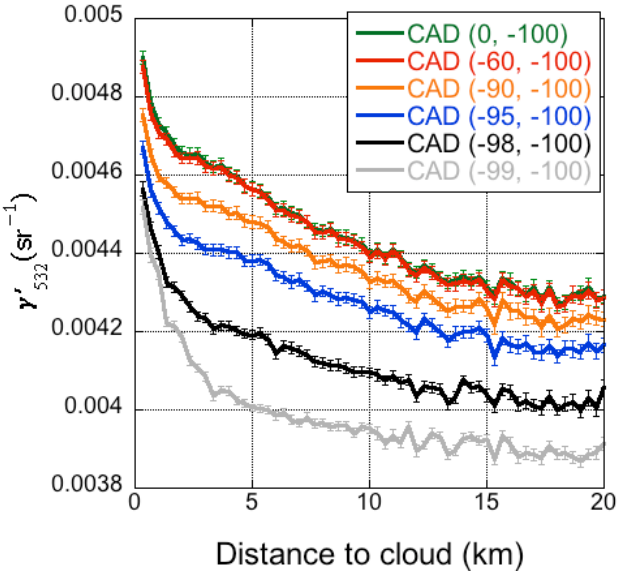

(a)

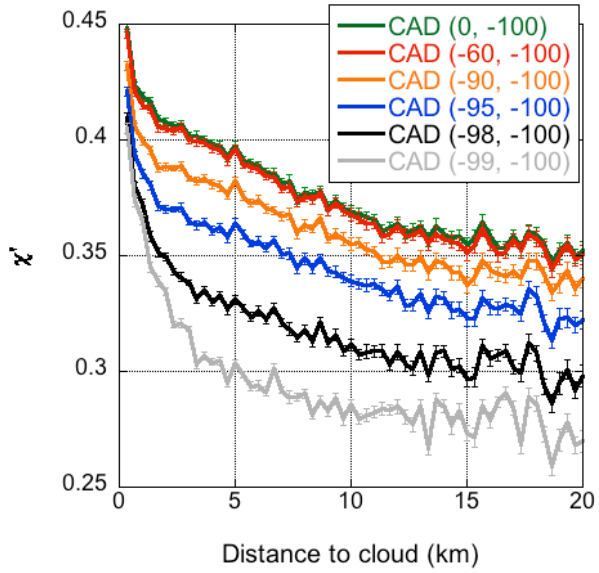

(b)

Figure 3. CAD-dependent backscatter behavior as a function of distance to clouds. (a) Integrated total attenuated 532 nm backscatter γ'_{532}. (b) Total attenuated color ratio χ'.

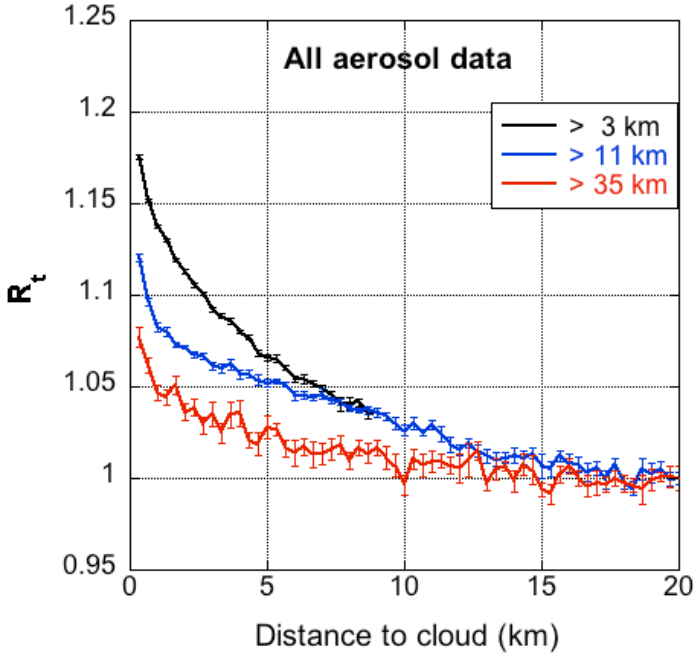

(a)

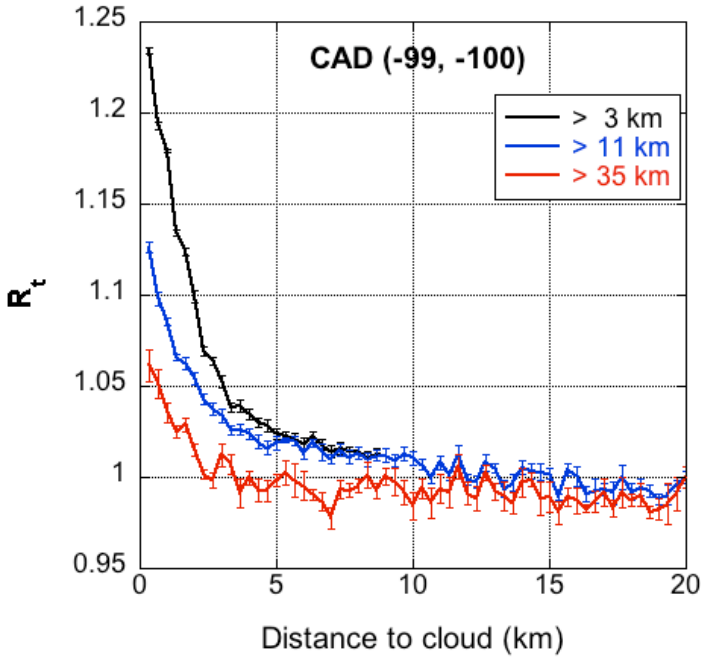

(b)

Figure 4. Normalized backscatters $R_t(x)$ near clouds, for three clear-sky segments > 3 km, > 11 km and > 35 km, respectively. (a) all aerosol data and (b) highest confidence level data CAD=(-99, -100).

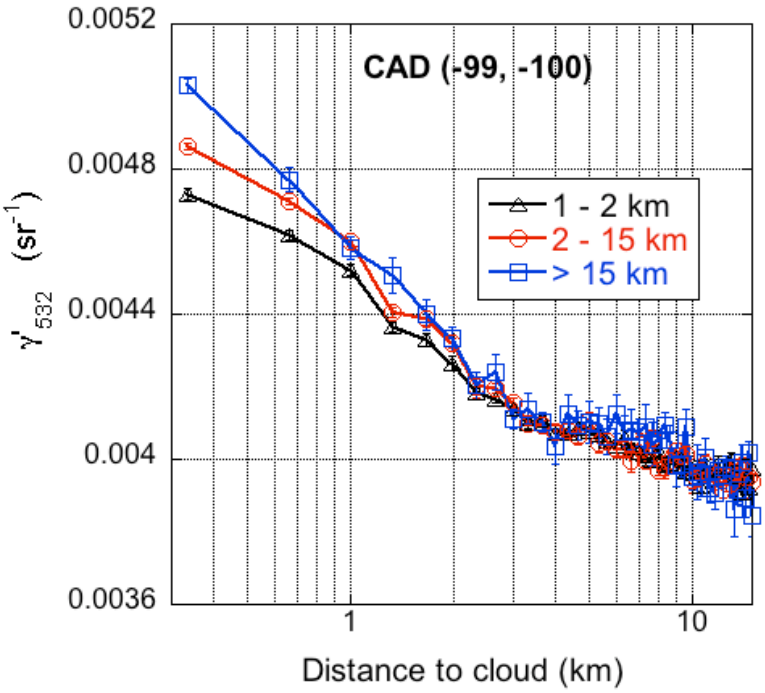

Figure 5. Near-cloud behavior of γ'_{532} for highest confidence level data, for different horizontal cloud sizes of 1-2 km, 2-15 km and larger than 15 km. The horizontal axis is in logarithm scale. To reduce uncertainties, a longer dataset (from June 20 to Aug. 31, 2007) is used for this figure.

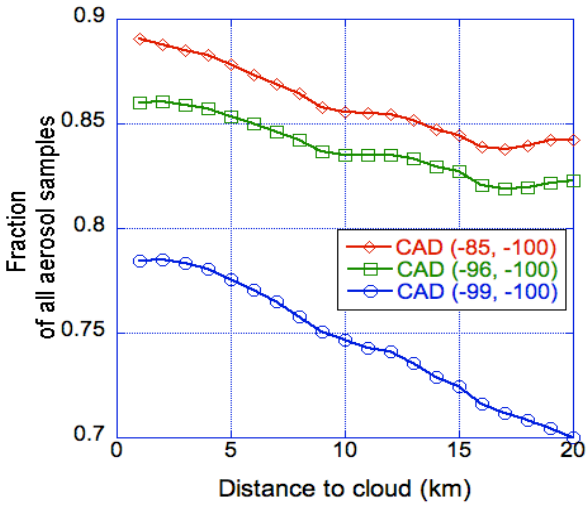

Figure A1. Fraction of high confidence level data as a function of distance to clouds for V3 data.